FERMILAB-PUB-24-0063-CSAID

The Design and Construction of the CHIPS Water Cherenkov Neutrino Detector

B. Alonso Rancurel[b], N. Angelides[e], G. Augustoni[b], S. Bash[1a,*], B. Bergmann[c], N. Bertschinger[d], P. Bizouard[a], M. Campbell[a], S. Cao[s], T. J. Carroll[d], R. Castellan[a], E. Catano-Mur[n], J. P. Cesar[l], J. A. B. Coelho[v], P. Dills[ab], T. Dodwell[a], J. Edmondson[a], D. van Eijk[g], Q. Fetterly[d], Z. Garbal[b], S. Germani[a,w], T. Gilpin, A. Giraudo[b], A. Habig[k], D. Hanuska[d], H. Hausner[i], W. Y. Hernandez[d], A. Holin[t], J. Huang[r], S. B. Jones[a], A. Karle[p], G. Kileff[a], K. R. Jenkins[a], P. Kooijman[g], A. Kreymer[i], D. A. Loving[n], G. M. LaFond[d], K. Lang[l], J. P. Lazar[p], R. Li[j], K. Liu[x,y], P. Mánek[a,c], M. L. Marshak[m], J. R. Meier[m], W. Miller[m], J. K. Nelson[n], C. Ng[aa], R. J. Nichol[a], V. Paolone[u], A. Perch, M. M. Pfützner[a], A. Radovic[a,n], K. Rawlins[h], P. Roedl[d], L. Rogers[d], I. Safa[o], A. Sousa[q], J. Tingey[a], J. Thomas[a], J. Trokan-Tenorio[n], P. Vahle[n], R. Wade[f], C. Wendt[d], D. Wendt[z], L. H. Whitehead [2a], S. Wolcott[d], T. Yuan[p]

[a] *Department of Physics and Astronomy, University College London, Gower Street, London, WC1E 6BT, United Kingdom*
[b] *Aix-Marseille University, Science Faculty in Saint-Jérôme campus, 13013 Marseille, France*
[c] *Institute of Experimental and Applied Physics, Czech Technical University in Prague, Husova 240/5, 110 00 Prague 1, Czech Republic.*
[d] *Department of Physics, University of Wisconsin, Madison, WI 53706, USA*
[e] *Imperial College London, Physics Department, Blackett Laboratory, London SW7 2AZ, UK*
[f] *Avenir Consulting, Abingdon, Oxfordshire, UK*
[g] *Nikhef, Science Park 105, 1098 XG, Amsterdam, The Netherlands*
[h] *University of Alaska Anchorage, 3211 Providence Dr. Anchorage, AK 99508*
[i] *Fermi National Accelerator Laboratory, Batavia, IL 60510, USA*
[j] *School of Physics and Astronomy, Shanghai Jiao Tong University, MOE Key Laboratory for Particle Astrophysics and Cosmology, Shanghai Key Laboratory for Particle Physics and Cosmology, Shanghai 200240, China*
[k] *Department of Physics and Astronomy, University of Minnesota Duluth, Duluth, Minnesota 55812, USA*
[l] *Department of Physics, University of Texas at Austin, Austin, TX 78712, USA*
[m] *University of Minnesota, Minneapolis, Minnesota 55455, USA*
[n] *Department of Physics, William & Mary, Williamsburg, VA 23187, USA*
[o] *Department of Physics, Columbia University, New York, NY, USA*
[p] *Department of Physics and Wisconsin IceCube Particle Astrophysics Center, University of Wisconsin–Madison, Madison, WI 53706, USA*
[q] *Department of Physics, University of Cincinnati, Cincinnati, OH 45221, USA*
[r] *School of Physics and Astronomy, Shanghai Jiao Tong University, China*
[s] *Institute For Interdisciplinary Research in Science and Education (IFIRSE), ICISE, Quy Nhon, Vietnam*
[t] *Particle Physics Department, STFC Rutherford Appleton Laboratory, Harwell Campus, Didcot OX11 0QX, United Kingdom*
[u] *University of Pittsburgh, Pittsburgh, PA, 15260, USA*
[v] *Université Paris Cité, Astroparticule et Cosmologie, F-75013 Paris, France*
[w] *Dipartimento di Fisica e Geologia, Università degli Studi di Perugia, I-06123 Perugia, Italy*
[x] *Department of Physics, Sun Yat-sen University, 135 Xingang Xi Road, Haizhu District, Guangzhou, 510275*
[y] *Department of Physics, Tsinghua University, 30 Shuangqing Road, Haidian District, Beijing, 100084*
[z] *Department of Physics, University of Colorado, Boulder, Colorado 80309, USA*
[aa] *Department of Physics and Astronomy, Michigan State University, East Lansing, MI 48824, USA*
[ab] *Department of Mechanical Engineering, University of Wisconsin, Madison, WI 53706, USA*

Abstract

CHIPS (CHerenkov detectors In mine PitS) was a prototype large-scale water Cherenkov detector located in northern Minnesota. The main aim of the R&D project was to demonstrate that construction costs

[1] Now at: Technische Universität München, James-Franck-Straße, 85748, Garching, Germany
[2] Now at: Cavendish Laboratory, University of Cambridge, Cambridge CB3 0HE, United Kingdom

of neutrino oscillation detectors could be reduced by at least an order of magnitude compared to other equivalent experiments. This article presents design features of the CHIPS detector along with details of the implementation and deployment of the prototype. While issues during and after the deployment of the detector prevented data taking, a number of key concepts and designs were successfully demonstrated.

*Corresponding author
Email address: simeon.bash@ucl.ac.uk (S. Bash)

Contents

1. Introduction

Neutrino detectors are typically very large and therefore very expensive. Planned and future detectors will need to have masses of tens or even hundreds of kilotons (kt) to register significant event counts.

Water Cherenkov detectors, owing to their large footprint and common target volume, can be particularly affected by cosmic backgrounds which necessitates additional shielding. This is commonly resolved by constructing such detectors deep underground, adding significantly to the costs. As an example, the Hyper-Kamiokande project is projected to cost over $600m for a 258 kt detector or $2.3m per kt [1, 2].

The purpose of the CHIPS (Cherenkov Detectors In Mine Pits) project was to demonstrate, through the construction of a prototype detector, that the cost per kt for future water Cherenkov (WC) experiments could be lowered by an order of magnitude. To achieve this a 5 kt CHIPS detector would be deployed in a flooded mine pit, 707 km away and 7 mrad off-axis from the NuMI beam at Fermilab. Crucially the water in the pit would provide both the cosmic ray shielding and the mechanical support for the purified detector water volume, thus avoiding the need for expensive excavation and support structures. The use of commercial, off the shelf components, for water purification, planes of photomultiplier tubes (PMTs) and readout electronics,

would further reduce costs. In this paper we describe the main characteristics of the novel detector design along with selected details of their implementation.

2. Experimental Concept

The CHIPS concept uses a volume of purified water as the detector medium. The volume is enclosed in a light- and water- tight membrane, submerged in a much larger volume of water such as a lake or mine pit. The surrounding water volume provides both the mechanical support for the detector volume and the cosmic ray shielding overburden.

Compared to conventional WC detector designs, this architecture offers three key advantages. Firstly, since suitable bodies of water are more likely to occur naturally than deep caverns, expensive excavation is not required. Secondly, as the entire detector is submerged, the water volume outside supports the water volume contained inside. This means that support structures are only needed to maintain the detector's shape rather than support the kilotons of its internal mass. Thirdly, the detector could be largely constructed in its final form above ground and later deployed to its submerged location in one piece. The key drawback of this concept is that following deployment, the entire detector is under water including its instrumentation, rather than just the photo-sensitive parts of its sensors. This increases the difficulty of, and sometimes effectively prohibits post-deployment repairs or maintenance.

Despite the fact that WC neutrino detectors are usually constructed deep underground, considerable effort is still expended in data analysis, classifying events and eliminating cosmic rays from the signal. However, if the detector is focused only on neutrinos coming from an accelerator, significant background reduction is possible even for modest overburdens [3]. The NUMI neutrino beam at Fermilab produces neutrinos in 10 µs beam spills. It has been shown that using modern machine learning reconstruction techniques to identify the beam neutrinos, as little as 50 m of water overburden would be sufficient to discriminate between cosmic ray and neutrino beam events [4].

To further minimise construction, assembly and maintenance costs, the prototype detector used as many standardised off-the-shelf components and readily available building materials as possible. It was designed in such a way that non-specialists (including students) could perform the majority of the construction tasks safely. An overview of the detector concept can be seen in Figure 1.

3. The PolyMet Mine Site

The CHIPS prototype was located at Wentworth 2W (W2W), a disused iron quarry at the PolyMet mine site near Hoyt Lakes, Minnesota (shown in Figure 2a). At the time of construction, this pit was still used as a buffer for managing water levels across the larger PolyMet site. This meant that water was occasionally pumped between the W2W pit and other nearby mine pits to moderate their water levels and chemical composition.

The PolyMet site was uniquely useful to CHIPS for several reasons. Firstly, the abandoned and flooded W2W pit provided a suitably deep location (60 m) for the detector. Secondly, the existing infrastructure that

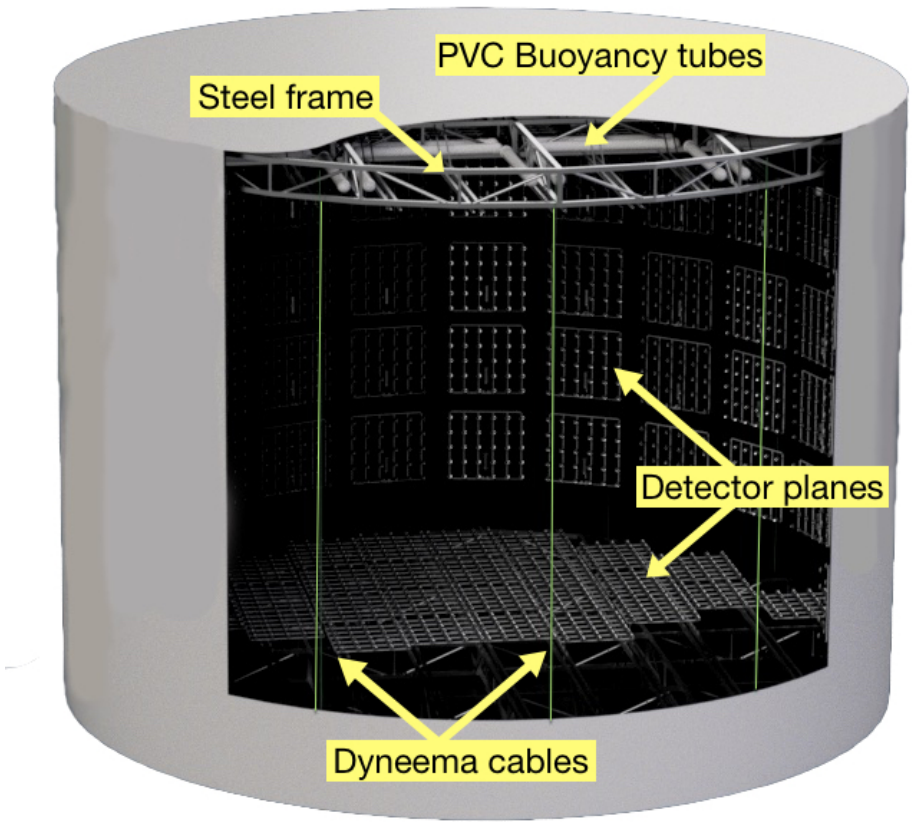

Figure 1: A rendering of the fully deployed CHIPS detector concept showing the overall structure: two steel end caps surrounding a cylindrical volume. The top cap is buoyant because of the PVC buoyancy tubes, whereas the bottom cap sinks, exerting tension on the vertical cables. The light-tight liner encloses the detector, protecting instrumented planes from undesirable incoming light. In addition to horizontal planes installed at the time of deployment, the rendering also shows vertical planes, which were envisioned to be installed during a future upgrade along the curved interior wall.

was maintained for future mining operations included road and rail connections, despite the remoteness of the location. This permitted easy access for heavy machinery and construction industries. The location of the mine site itself was important; the site was within an accessible distance to the Soudan Underground Laboratory Surface Building, which supplied large equipment and tools. Finally, and most importantly, the site was in the path of the NuMI beam as it re-emerged from the Earth (shown in Figure 2b).

The construction of CHIPS exploited the changes of the mine pit's controlled water levels. This allowed the detector to be built on dry land, which was later flooded prior to deployment (this is described in detail in Section 5). The detector and its elements were constructed on a slipway at the edge of the mine pit as shown in Figure 3. Adjacent to this location, two huts were erected to house a water treatment plant and electrical equipment respectively. Space inside the PolyMet main building was dedicated to preparation of computing equipment and light-sensitive instrumentation.

4. Mechanical structure

The CHIPS detector was mechanically supported by a metal frame comprising two (25 m) diameter circular end caps. To achieve a high strength-to-weight ratio, both caps relied on lattice frame construction. As the structure was expected to be submerged in water for extended periods of time, stainless steel was selected because its corrosion resistance would prevent rust from degrading water clarity in the internal volume. Components of the frame's main structure can be seen in Figure 4. Rather than manufacturing perfect circles, the end caps were rigid icosikaioctagon (28-sided regular polygons) steel frames. Steel beams, known as *stringers*, were mounted facing the interior of the cylinder in parallel rows, to which the instrumentation would be attached as shown in Figure 5. Overall each steel end cap weighed 14 t.

Before deployment, the frame was fabricated off-site and shipped in pieces to the mine pit. Each piece was assembled with a single telescopic forklift. Stringers could be moved by two workers. This meant that, including the forklift operator, the frame could be assembled by a team with as few as three people.

Both end caps were constructed on top of each other. First, the bottom cap was built on the ground supported by rubber tyres, visible in Figure 4. The bottom cap had 92 stainless steel pegs distributed approximately uniformly across the detector pointing upwards; hollow stilts made of steel tubing were mounted on top of these pegs visible in Figure 6. The top cap was built sitting on top of the stilts. During construction, PVC tubes were installed to provide approximately 15 t of flotation which made the top cap net buoyant in water as shown in the top of Figure 19.

The completed frame is displayed in Figure 6. Following deployment, the two caps were no longer rigidly attached to each other, since the bottom cap sank while the top cap floated.

In order to accurately measure relatively faint Cherenkov light, the internal detector volume needed to be clear, dark and well-isolated from external light sources. To this end, the detector was fully enclosed

(a) Map showing the locations of the NuMI beam source at Fermilab, the W2W mine pit, where CHIPS was located, and other neutrino detectors (MINOS and NOvA). [5].

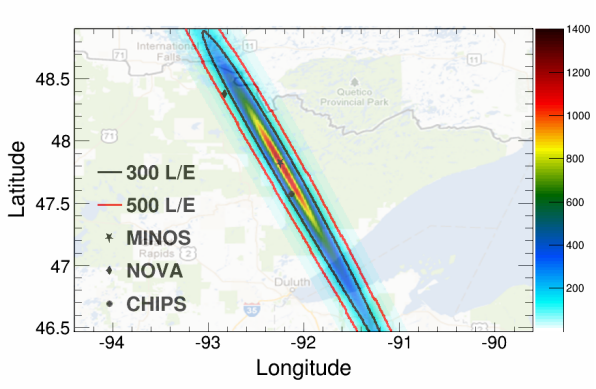

(b) A map of the NuMI beam exiting the Earth's surface showing the positions of CHIPS, NOvA and MINOS. The color axis shows the expected number of neutrino events per year per kiloton of water assuming no neutrino oscillations. Contours of constant L/E are shown. Image taken from [6].

Figure 2

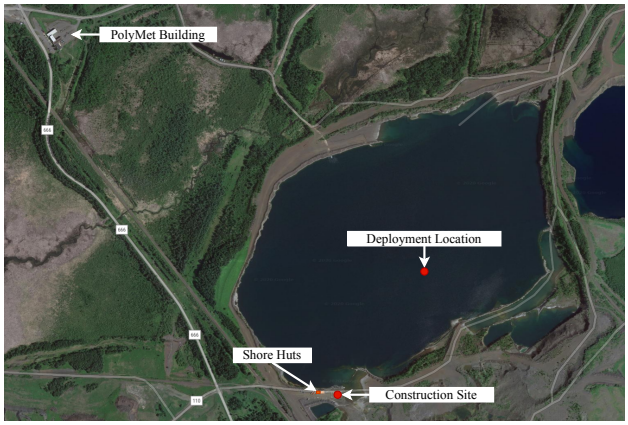

Figure 3: The PolyMet mine site. CHIPS was built beside the mine pit on a flat construction area with additional assembly done in the PolyMet building.

Figure 4: Components of the bottom end cap. The gusset plates that were used to join pieces together are visible, as are the tyres that support the frame. The hollow lattice reduces weight, as less steel is required than for a solid detector.

Figure 5: Rows of stringers bolted onto the main support structure. Instrumentation would be attached onto the top of the stringers.

Figure 6: Completed frame. The pillars supporting the top cap are clearly visible.

in a geomembrane liner. In addition to providing a light seal, this barrier also implemented the separation between internal, filtered water and external pit water, which contained impurities and wildlife. In addition, during deployment the liner would act as a hull that allowed the detector to remain dry inside, float due to water displacement and move like a boat (see Section 5 for details).

The liner was crafted from flexible fibre-reinforced plastic (XR-5 Geomembrane [7]), conventionally used for roofing. This material provided sufficient strength as well as light- and water-tight properties. The membrane was delivered in 2.54 m wide, 183 m long rolls. Following construction of the supporting frame, the liner was installed in individual strips, which were heat-fused using specialist welding equipment to form the skin of a 25 m diameter, 12.5 m tall closed cylinder. Since the height of the detector was expected to increase during deployment, the liner was pooled at the base of the detector.

5. Structure summary and deployment procedure

The steel frame, the liner, the water and the flotation all worked together to give the CHIPS detector its final structural form. The frame gave the cylinder its rigid round cross-sectional shape and acted as a mounting platform for detector planes. The height of the detector was determined by both the liner and the Dyneema cables, which limited the largest possible distance between end caps. Since the detector was filled with water and was itself submerged underwater, the water on the outside of the detector supported the weight of the water inside its volume. This meant the frame only needed to bear its own weight and the weight of the instrumentation attached to it.

The deployment procedure was planned as follows:

1. The detector would be built on dry land and sealed.
2. External floats surrounding the detector would be attached to support the detector during deployment
3. The detector would be towed by boat to its deployment location (shown in Figure 7).
4. The umbilical pipe containing the power and data connections would then be connected to the pass-through plate. The two high-density polyethylene (HDPE) pipes for circulating the water would also be connected so that water could be added and removed from the detector using electric pumps.
5. The detector would then be filled with water from the mine pit. This would cause its bottom cap to sink while the top cap remained on the surface. Consequently, the detector height would start increasing as more water was added. This process would continue until the Dyneema cables were under tension and the detector reached its maximum height.
6. Finally, the detector would be lowered to the bottom of the mine pit using external floating winches attached to the external float assembly. The weight of the bottom cap would keep the detector in place; the buoyancy of the top cap would keep the top cap floating above the bottom cap to give the

Figure 7: The detector, towed from the construction site to the deeper water.

Figure 8: The interior of the water hut showing the filtration plant.

detector its height. Overall the detector would remain sunken. At this point, the detector would be fully deployed.

6. Water Purity

To maintain the water's optical clarity inside the detector, the water had to be filtered. A filtration plant was housed in a hut on the shore of the pit. The hut housed ten pairs of 10 µm carbon block filters and 0.5 µm polypropylene filters installed in parallel (shown in Figure 8).

Water was to be pumped from the detector through the filters and back to the detector with a submerged pump through HDPE pipe. Two lengths of HDPE pipe were prepared by butt welding segments together until

Figure 9: The completed inflow and outflow water pipes for the detector. The third, shorter pipe is the water intake from the mine pit, which was used for filling the detector during deployment.

each was over 300 m long. During nominal operation, the water system formed a closed loop, so the water could be continuously cycled through the filters. To fill the detector for the first time during deployment, the water had to be pumped into the detector from the lake via the filtration plant.

Laboratory prototyping indicated that attenuation lengths in excess of 100 m were achievable with this system starting from samples of pit water [8, 9], significantly larger than the 25 m detector diameter. The system was designed to pump up to half a million litres per day; this was achieved during testing. At such rate, the full detector volume would pass through the filters approximately every two weeks. Generally, about 7 turnovers are required in order to ensure that 99% of the water actually passes through the filters [10]. This would lead to complete filtering of the detector water every 3 to 4 months.

7. Detector Planes

To observe Cherenkov light produced by neutrino interactions in water, the detector was instrumented with 2000 PMTs arranged into small rectangular detector planes, each carrying approximately 30 PMTs. These detector planes provided a modular and rigid mounting system for the PMTs in manageable numbers and also a waterproof connection to the readout and data acquisition (DAQ) electronics.

The detector planes consisted of a frame made of rungs of standard plumbing PVC pipe. At the centre of the frame was a cylindrical container, which housed electronics, and across the frame, pointing outwards, were plumbing fixtures, where PMTs were installed. Each PMT would be sealed inside a plastic insert that was glued to the frame, from there it was connected to readout electronics using a standard CAT-5 cable. This provided all of the necessary power and signalling. A rendering of a detector plane can be seen in Figure 10.

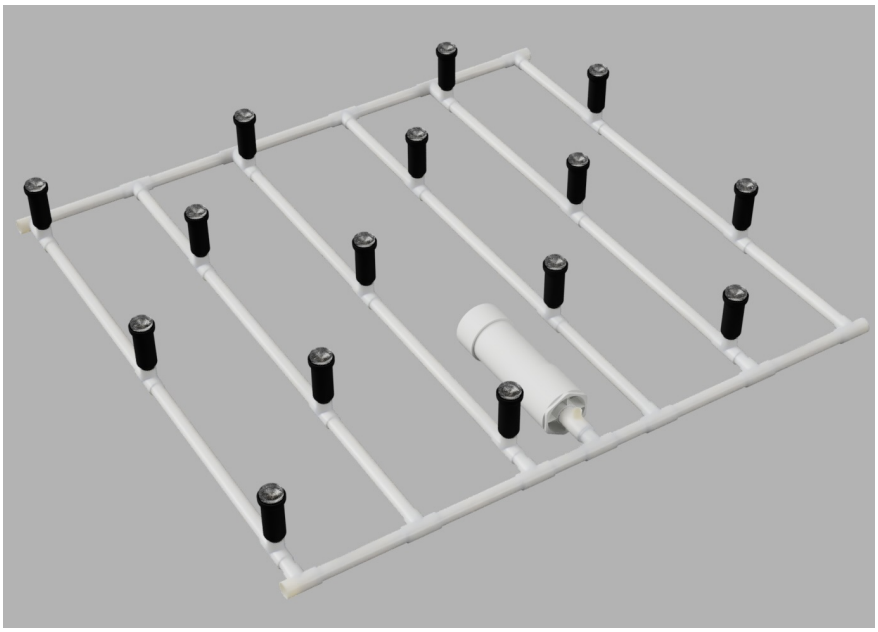

Figure 10: Rendering of a detector plane. The PMTs are housed inside the custom plastic inserts (black). The inserts are glued into standard 'tee' fittings which are part of the PVC frame (white). The electronics container in the centre is also made from PVC. CAT-5 cables connect each PMT to readout electronics inside the container.

In order to detect photons, PMTs require high voltage (HV). In CHIPS, each PMT generated HV in situ using a dedicated base that implemented a Cockroft-Walton (CW) voltage multiplier. This meant that no large central HV supply was required and no HV cabling was necessary. PMT bases also digitised measured analog signals, which were distributed up-stream to each plane's DAQ electronics. The only connection between each PMT and the electronics container was the single CAT-5 cable.

Since detector planes were composed of standard PVC plumbing pipes and fixtures, their assembly was greatly simplified. Waterproof seals were achieved using commercially available PVC primer and cement. This was desirable in practice, as assembly could be performed on-site without specialist staff.

There were distinct two kinds of detector planes in CHIPS, named after the locations at which they were created:

- Nikhef planes: based on KM3NET electronics [11] modified for the CHIPS geometry. These planes carried HZC photonics `XP82B20FNB` PMTs, which used a negative HV supply. Consequently, during nominal operation the PMT face would become energized, and could not come into contact with water.
- Madison planes: designed by CHIPS at the University of Wisconsin-Madison in conjunction with the IceCube experiment [12]. These planes carried Hamamatsu `R6091` PMTs, which used positive HV supply. This meant that during operation there was no potential difference between the photocathode and the water.

Figure 11: The photocathode of a Madison PMT exposed to the environment. The tube was glued into the plastic insert (white) with a resin potting compound (black). This created a waterproof seal between the glass and the plastic.

Since the faces of the PMTs in the Madison planes came into contact with water, a positive HV was applied via a CW base (rather than a negative HV). Custom PVC inserts, which were sealed with a watertight potting compound as shown in Figure 11. This allowed PMTs to be exposed to the detection medium with no barriers or interfaces, yet the rest of the PMT electronics and the plane were fully protected by a watertight seal. In contrast, PMTs of Nikhef planes were fully insulated from the water owing to their negative polarity HV. In order to minimize undesirable optical properties, acrylic was used as a transparent insulator. The PMTs were placed in a custom PVC insert and a transparent acrylic cover with a water sealing O-ring was bolted to the front. This insulated the photocathode at HV from the earthed water. Finally, a reflective cone was attached to the cover which increased the light collection efficiency by 60%. The constituent parts of the assembly can be seen in Figure 12 and the final assembled PMT can be seen in Figure 13.

To reduce optical losses due to reflection and refraction at the optical interface between the cover and the glass face of Nikhef PMTs, the glue that permanently joined these components was carefully selected to match their refractive index. It was critical that the glue was applied with no contamination, imperfections or bubbles. Furthermore, due to its relatively high cost it was desirable to minimise the amount of applied glue per PMT. The attachment of a PMT cover was performed as follows. First, 15 ml of potting compound was deposited inside an acrylic cover, into which a PMT (shown in Figure 14a) was placed face down. A dedicated jig was developed to hold the PMT upright, allowing the tube to move vertically. The natural

Figure 12: Disassembled Nikhef PMT. From the left: plastic insert, the PMT itself with its HV base attached, the waterproof cover complete with its O-ring, and finally the plastic light reflector.

Figure 13: Assembled Nikhef PMT, ready to be glued onto a plane.

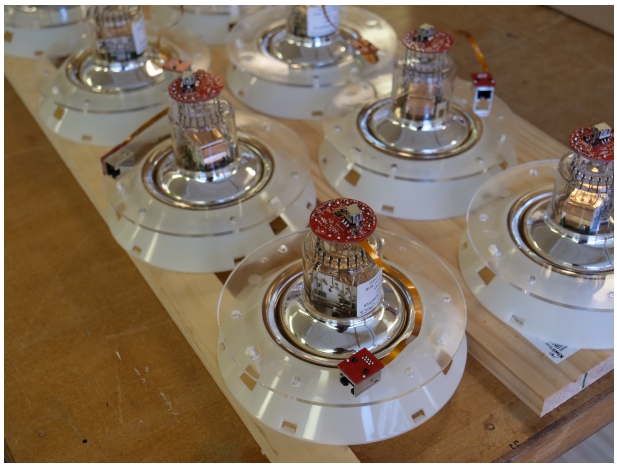

(a) PMTs after the stabilising jig had been removed. The PMT covers are oriented towards the ground, so that each PMTs can be seated inside its cover.

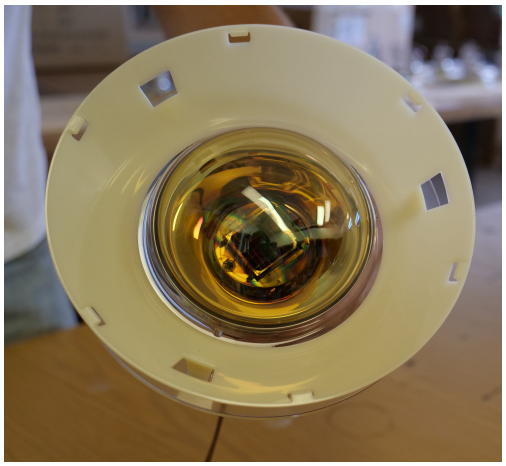

(b) A potted Nikhef PMT. The presence of the optical glue between the plastic and the glass reduced the reflectivity between the two layers. The acrylic cover electrically insulates the face of the PMT from its surrounding environment.

Figure 14

buoyancy lifted the PMT slightly above the plastic, allowing the glue to occupy the space between the two media. The use of buoyancy of the PMT elegantly removed the need for complex supporting structures that would hold the PMT at a precise height, as the buoyancy of the tube was reliable and reproducible. This method produced 225 potted PMTs a day, which was performed by a team of students. A completed PMT can be seen in Figure 14b.

In total, 62 planes were placed into the detector, 56 Nikhef planes spread out between the top and bottom caps, and 6 Madison planes in just the bottom cap. Approximately 60 more Nikhef planes and 24 more Madison planes were prepared for a detector upgrade which would have increased the PMT coverage in the detector. An example of a completed plane installed inside the detector can be seen in Figure 15.

Figure 15: Completed Nikhef plane installed in the detector. Each PMT has an acrylic cover and reflector attached. The PMTs are sealed inside their inserts and installed into the PVC plane frame. The electronics container located in the centre of the plane. A flexible PVC hose (incomplete) exits the electronics container, which would connect the plane to upstream power supplies and DAQ electronics.

8. Electronics and Timing

Each detector plane type was operated using dedicated DAQ electronics. Madison planes used a microprocessor-based MicroDAQ board [12] mounted on individual PMTs to digitise, timestamp, record and distribute observed signals. At the centre of each plane was a fanout board which simply aggregated data streams from all MicroDAQs and multiplexed them into the detector network.

Nikhef planes also used intelligence mounted on the PMT bases to digitise signals and fanout boards to aggregate data. However, in contrast Nikhef bases were less autonomous than MicroDAQs. This meant that a lot of functions performed by MicroDAQs were carried out by the fanout board instead (for instance, hit timestamping). These electronics were purchased from KM3NeT (with different connectors) and can be seen in references [13, 14, 11].

To integrate heterogeneous detector planes into a single distributed measuring system, a second level of fanout boards was introduced. These were housed in dedicated electronics containers, which were physically distributed within the detector. Each of these containers housed power and data network infrastructure implemented by White Rabbit (WR) switches [15] [16]. This was a 1 Gbit fibre optic Ethernet network (consisting of single-mode fibres and wavelengths of 1310 nm and 1550 nm), which served a dual purpose: in addition to carrying conventional data packets it transmitted precise time signals, which allowed individual sensing components of the detector to be synchronised within 100 ps. The network coalesced at a central electronics container, which was responsible for power switching and facilitating the master data link to the shore via umbilical that was terminated at a hut on the shore. Inside the hut, a cluster of Linux computers

controlled the detector, monitored its state and saved data. Also on the shore was a GPS antenna with a receiver connected to a WR grandmaster clock that provided absolute time reference.

Implementation of the timing synchronisation and distribution system is beyond the scope of this paper. See [17].

9. Detector Deployment and Lifecycle

The CHIPS detector was deployed in October 2019, as shown in Figure 16. During deployment, the liner sustained damage during the towing procedure prior to water ingress. This prevented the detector interior from maintaining full buoyancy. Consequently, the float-mounted winches were supporting the full load without the advantage of additional flotation from the detector itself and partial failure of the winch system followed. The outcome was that the detector could not be fully deployed as planned before the winter. The liner was to be repaired in spring the following year when the lake thawed.

Figure 16: The exterior of the detector after completion. The liner can be seen supporting the detector and the floating dock forms a perimeter around the detector. Two boats tow and steer the detector during deployment. The scale of the detector is visible.

In March 2020, the COVID-19 pandemic halted all access to the site. During spring and summer, the structural condition of the system further deteriorated. Several months later, in September the detector was removed from the water as there was no clear timeline to resume activities and the pandemic had not resolved.

In spite of mechanical damage that prevented its full deployment, the detector was put into limited operation for a short period of time. During that time, it underwent various technical checks that demonstrated its viability ahead of planned commissioning. For instance, the control and monitoring system, trigger and time distribution systems were successfully tested in late 2019. Furthermore, both DAQ software as well as electronics were used to take data after deployment was aborted. An example of a hitmap for a cosmic

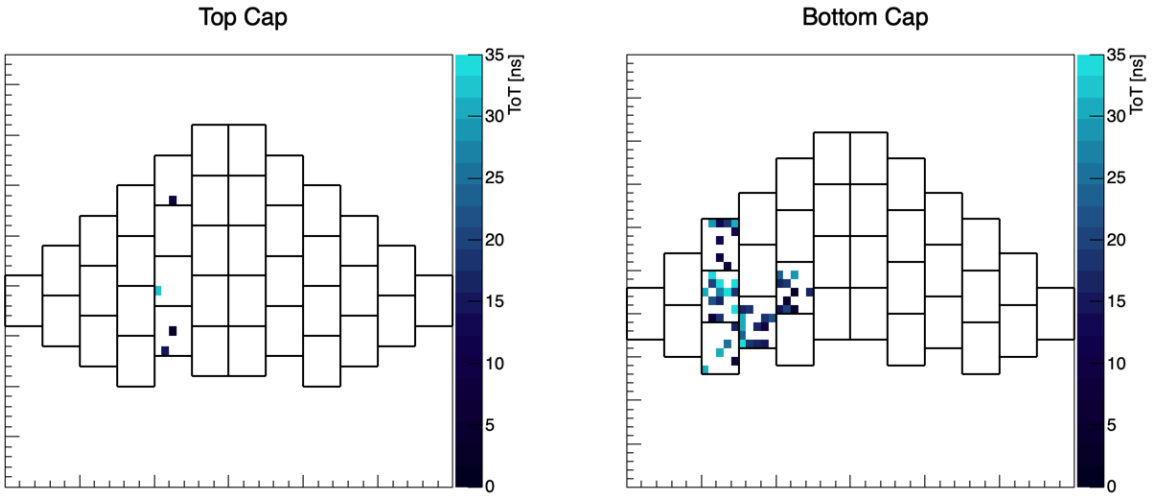

Figure 17: A CHIPS hitmap (the detector from above) showing what is likely to be a cosmic ray muon event. The damage sustained to the detector during deployment gave little time to assess detector efficiency. This event is assumed to be a cosmic ray as it is unlikely to be noise because each plane had been tested before installation to ensure low noise. At the time of this event, the NuMI beam was not running.

ray event can be seen in Figure 17 which demonstrated that the detector was operational after deployment. Figure 18 shows the number of PMTs registering hits inside a time window of 30 ns for different hit number thresholds.

Following its removal, the detector was disassembled in such a way that permitted its instrumentation to be reused for future projects. The mine site was returned to its original state.

10. Conclusion

The CHIPS R&D project aimed to demonstrate that significant cost reduction could be achieved in construction of WC neutrino detectors. To this end, a prototype was designed and built using widely available and inexpensive components. Its assembly and deployment were carried out in a disused mine pit with a workforce that, on the whole, was non-specialist. During project realisation, a variety of cost-saving methods were tested, refined and shown to be viable for large-scale application. Consequently, the total cost of the hardware components for the prototype was estimated to be €1.7m which could have equipped 15 kt if the detector had been expanded fully. Despite not observing accelerator neutrinos during its relatively short lifespan, the detector's instrumentation passed numerous internal tests, indicating its suitability for future scientific operation and demonstrating the capability to observe directed light in a large-scale WC detector. The total cost of the hardware is estimated to be on approximately

In summary, the construction of the CHIPS prototype entailed broad exploration of the landscape of

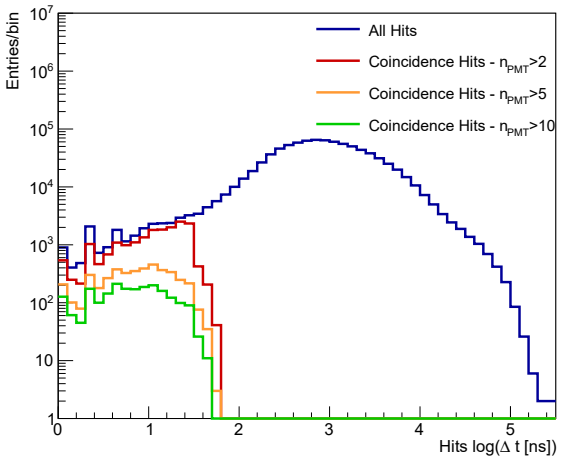

Figure 18: Time window length between two successive hits as a function of number of PMTs hit for different hit number thresholds. The noise is clearly seen in blue above a two hit window length of 30 ns, (note logarithmic scale) whereas the actual coincidences can be seen below that.

cost reduction strategies, which could be potentially employed beyond the scope of this project in future low-cost neutrino detectors. In that sense, even though the prototype did not observe NuMI neutrinos, vast majority of goals set for this project were satisfied at the time of its deployment. The prototype detector was assembled and deployed from April to October 2019. The detector was decommissioned in July 2020. Its instrumentation is currently reused for other research projects.

11. Acknowledgements

This work was supported by Fermilab; the Leverhulme Trust Research Project Grant; U.S. Department of Energy; The Royal Society Research Professorship funding for J.Thomas and the European Research Council funding for the CHROMIUM project.

The CHIPS collaboration would like to thank the Wisconsin IceCube Particle Astrophysics Center, University of Wisconsin–Madison, University College London, University of Alberta, University of Minnesota Duluth, Aix-Marseille University. Additionally, the CHIPS collaboration would like to thank PolyMet and Cleveland-Cliffs for hosting the experiment.

Fermilab is operated by Fermi Research Alliance, LLC, under Contract No. DE-AC02-07CH11359 with the U.S. DOE.

Figure 19: The interior of the detector: the rows of Nikhef PMTs angled to point into the neutrino beam can be seen. The narrow height between the bottom and top caps before the expansion during deployment is visible. Image courtesy of Albrecht Karle.

References

[1] D. Castelvecchi, Japan Will Build the World's Largest Neutrino Detector, Nature (12 2019). doi:10.1038/d41586-019-03874-w.

[2] F. Di Lodovico, The Hyper-Kamiokande Experiment, Journal of Physics: Conference Series 888 (2017) 012020. doi:10.1088/1742-6596/888/1/012020.

[3] D. S. Ayres, G. R. Drake, M. C. Goodman, et al., The NOvA Technical Design Report (10 2007). doi:10.2172/935497.

[4] J. Tingey, S. Bash, J. Cesar, et al., Neutrino characterisation using convolutional neural networks in CHIPS water Cherenkov detectors, Journal of Instrumentation 18 (06) (2023) P06032. doi:10.1088/1748-0221/18/06/P06032.
URL https://dx.doi.org/10.1088/1748-0221/18/06/P06032

[5] Esri. "topographic" [basemap]. Scale Not Given. "world topographic map". january 12, 2023 [online] (1 2023).

[6] P. Adamson, J. Austin, S. V. Cao, others., CHerenkov Detectors In Mine PitS (CHIPS) Letter of Intent to FNAL, Tech. rep., Fermi National Accelerator Laboratory (FNAL), Batavia, IL (United States) (12 2013). doi:10.2172/1342789.

[7] Seaman Corporation, XR Geomembranes, accessed 5 June 2023 (6 2023).
URL https://www.xrgeomembranes.com

[8] M. Campbell, Measuring Neutrino Oscillations in the NOvA and CHIPS Detectors, Ph.D. thesis, University College London (2020).

[9] F. Amat, P. Bizouard, J. Bryant, et al., Measuring the attenuation length of water in the CHIPS-M water Cherenkov detector, Nuclear Instruments and Methods in Physics Research Section A: Accelerators, Spectrometers, Detectors and Associated Equipment 844 (2017) 108–115. doi:10.1016/j.nima.2016.11.032.

[10] S. Battersby, Clay's Handbook of Environmental Health, Routledge, 2022. doi:10.1201/9781003035640.

[11] A. Margiotta, A. Marinelli, C. Markou, et al., KM3NeT Front-End and Readout Electronics System: Hardware, Firmware, and Software, Journal of Astronomical Telescopes, Instruments, and Systems 5 (04) (2019) 1. doi:10.1117/1.JATIS.5.4.046001.

[12] T. Huber, J. Kelley, S. Kunwar, et al., The IceTop Scintillator Upgrade, in: Proceedings of 35th International Cosmic Ray Conference — PoS(ICRC2017), Sissa Medialab, Trieste, Italy, 2017, p. 401. doi:10.22323/1.301.0401.

[13] D. Gajanana, V. Gromov, P. Timmer, ASIC Design in the KM3NeT Detector, Journal of Instrumentation 8 (02) (2013) C02030–C02030. doi:10.1088/1748-0221/8/02/C02030.

[14] D. Real, D. Calvo, Digital Optical Module Electronics of KM3NeT, Physics of Particles and Nuclei 47 (6) (2016) 918–925. doi:10.1134/S1063779616060216.

[15] M. Lipiński, T. Włostowski, J. Serrano, et al., 2011 IEEE international symposium on precision clock synchronization for measurement, control and communication, in: White rabbit: a PTP application for robust sub-nanosecond synchronization, 2011, pp. 25–30. doi:10.1109/ISPCS.2011.6070148.

[16] T. Włostowski, Precise time and frequency transfer in a white rabbit network, Master's thesis, Warsaw University of Technology (2011).

[17] S. Bash, J. Cesar, G. Deuerling, et al., Low-Latency NuMI Trigger for the Chips-5 Neutrino Detector, Nuclear Instruments and Methods in Physics Research Section A: Accelerators, Spectrometers, Detectors and Associated Equipment 1030 (2022) 166513. doi:10.1016/j.nima.2022.166513.